Article

JOURNAL OF COMPOSITE MATERIALS

Journal of Composite Materials
0(0) 1–16

DOI: 10.1177/0021998320964263
journals.sagepub.com/home/jcm
SAGE

Effect of MWCNT carboxylation on mechanical, thermal and morphological behaviour of phenol formaldehyde nanocomposites

Lakshmipriya Ravindran[1,2], MS Sreekala[2], S Anilkumar[1] and Sabu Thomas[3]

Abstract

Phenol-formaldehyde resin is an inevitable polymer material because of their excellent properties like heat resistance, chemical resistance, creep resistance, and low water sorption. But the drawback associated with PF matrix is buckling and brittleness. The incorporation of nanofillers can effectively reduce these problems. Carbon nanotubes is one among the nanofiller which is widely used to enhance the mechanical, thermal, electrical properties of the host matrix.The present study deals with the synthesis and comparison of two Phenol-formaldehyde nanocomposites incorporated with pristine multiwalled carbon nanotubes and carboxylated multiwalled carbon nanotubes via in-situ polymerisation technique. The effect of filler loading (MWCNT, MWCNT-COOH) with different weight percentages (0.05 wt%, 0.08 wt%, 0.12 wt%, 0.15 wt%) has been investigated in this study. Pristine MWCNT was functionalised with carboxyl groups and confirmed by XRD, FT-IR, CHN analysis, X-ray photoelectron spectroscopy, AFM and Raman spectra. All these analysis showed successful funtionalisation of pure MWCNT. The prepared nanocomposites were compared by mechanical, thermal and morphological analysis. The effect of both fillers on tensile strength, stress-strain, young's modulus and elongation at break were also analysed. The addition of MWCNT and MWCNT-COOH have enhanced the mechanical and thermal properties of the prepared nanocomposite. The mechanical properties of PF-MWCNT nanocomposite showed a maxima for 0.12 wt% and for PF-MWCNTCOOH nanocomposite it was 0.08 wt%. Higher thermal stability was exhibited for 0.15 wt% MWCNT loading. The thermal stability enhanced by the addition of MWCNT COOH upto 0.12 wt% and then declined. Moreover the prepared nanocomposites were morphologically characterized by scanning electron microscope (SEM) and transmission electron microscope (TEM) and from the fracture analysis it is clear that the reinforcements brought plastic deformation of phenol-formaldehyde nanocomposite from brittle to more ductile material. From the TEM image it was clear that the presence of carboxyl groups attached on MWCNT reduced agglomeration in PF matrix. Halpin-Tsai modelling was done for comparing experimental and theoretical values of tensile modulus and it illustrates good correlation.

Keywords

Phenol-formadehyde resin, MWCNT, MWCNTCOOH, mechanical, thermal, morphological analysis

Introduction

In recent years polymer based nanocomposites received much attention as it shows excellent enhancement in properties compared to the pure polymer. For the past 20 years the field of nanotechnology has emerged very vastly. The materials with nanoscale dimensions exhibit unique properties which are not found in the macro materials. The incorporation of these nano additives into a polymer will improve its desired properties.

[1]Postgraduate & Research Department of Chemistry, N.S.S Hindu College, India
[2]Postgraduate & Research Department of Chemistry, Sree Sankara College, India
[3]School of Chemical Sciences, Mahatma Gandhi University, India

Corresponding author:
MS Sreekala, Postgraduate & Research Department of Chemistry, Sree Sankara College, Kalady, Kerala 683574, India.
Email: sreekalams@yahoo.co.in

Carbon nanotubes are one among the nanoadditives which found many applications in the field of nanocomposites. The synergetic effect of nanoadditives and host matrix can bring increase in mechanical, thermal and electrical properties. Due to the excellent optical, electrical, and mechanical properties of carbon nanotubes, it has received much attention among the researchers.[1–3]

Carbon nanotubes was first discovered by M .Endo in 1978 during his Ph.D work and Iigima reported first in 1990, from that onwards it has got great attention.[4,5] It has many applications like nanoelectronics[6] photovoltaic cells,[7] superconductors,[8] electrochemical capacitors,[9] nanocomposites[10] and sensors.[11] CNTs are one of the allotropes of carbon which are cylinders of graphite that are covalently bonded. Since CNT is composed of sp^2 carbons which is very strong compared to sp^3 carbons which is the reason for its high mechanical properties. The advantage associated with CNT is the small dimension which makes it as a perfect reinforcement for improving the mechanical and thermal properties of polymer matrix. CNT exhibits very good mechanical property with a Young's modulus of 0.27 - 0.95TPa.[12] Large number of works are still going on in the field of both thermosetts and thermoplastics reinforced with CNT. Several research studies are going on in polymer reinforced CNT composites.[13–15]

Phenol formaldehyde resin is associated with applications in the field of aerospace, structural components, adhesive industry, foam materials etc.[16,17] By the incorporation of nanofillers these problems can be rectified. The history of phenol-formaldehyde (PF) resin relies on the invention of "Bakelite" by Leo Bakeland in 1907.[18] It was also called Bakelite and was the first synthetic plastic ever made. Being a nonconductive material PF resin has enormous usage in the field of electrical insulators, circuit board production moulding compounds, coating, adhesives etc. From the early stage onwards Bakelite was used as a matrix for making composites. Even though PF have excellent thermal stability, insulation properties, flame retardancy, ablation properties, its inherent nature is brittleness and buckling. The brittle nature of PF resin due to high crosslink density restricts its industrialisation. The phenol- formaldehyde resin has phenomenal chemical and physical properties compared to other plastics. PF resins are actually thermosetting polymers which can be obtained by treating phenol with formaldehyde. By incorporating nanofillers with PF resin shows excellent physical and chemical properties than from the pure form.

As indicated earlier PF polymers have excellent thermal stability, insulation properties, flame retardancy, ablation properties, its inherent nature is brittleness and buckling. These properties can be reduced by reinforcements with nano materials, toughners like rubber, incorporating elastomers etc. Alumina nanoparticle reinforced PF resin showed enhancement in curing rate and better interaction with the host matrix.[19] It is reported that the addition of CNT and graphene derivatives improved the mechanical properties and thermal stability of PF nanocomposite. PF resin modified different functionalities of graphene oxide improved the degradation temperature and char yield.[20] More over nano hybrids of graphene oxide and CNT enhanced the mechanical properties of PF matrix.[21]

The perfect reinforcing effect depends on high aspect ratio of the filler, uniform dispersion, and better interfacial interaction with the polymer matrix. For the efficient load transfer between the filler and polymer matrix homogenous dispersion plays a pivotal role. Otherwise the CNT's will tend to agglomerate leading to the degradation of properties. Out of different processing techniques we have adopted in-situ polymerisation technique since it can bring excellent interaction of CNT with polymer matrix. Abedi et al.[22] fabricated polyethylene-clay nanocomposite by in-situ polymerisation technique. A conducting polymer nanocomposite was prepared by reinforcing graphene oxide homogeniously via insitu polymerisation.[23] Several researchers have adopted this technique for attaining a homogenius dispersion of nanomaterials in polymer matrix.[24–28]

In the case of thermosetting polymers in-situ polymerisation is found to be an effective processing technique for attaining a homogenious dispersion of CNT in the polymer. Moreover the funtionalisation of CNT can bring effective interaction and better compatibility with the polymer matrix. The sidewalls of CNT can be carboxylated by oxidative treatments with acid mixtures. The commonly used acid mixtures are HNO_3, HNO_3 – H_2SO_4, $KMnO_4$, H_2O_2, $KMnO_4$-H_2SO_4.[29–36] The oxidative treatments modifies the sidewalls of the CNT with carboxyl group (-COOH) and hydroxyl group (–OH). Several researchers have adopted these oxidative treatments for surface funtionalisation of CNT.

Several works are going on to improve the properties of PF composites. The application of PF resin as composites mainly relies on the presence of intermolecular hydrogen bonding. These will help to interact strongly with functional groups present in the fillers. Zhang and co-workers developed phenolic composite incorporated with boron and silicon in order to improve heat resistance and anti-oxidation property.[37] Thermal stability of epoxidised phenolic resin was increased by the addition of graphene oxide derivaties.[20] The effect of CNT reinforcement on phenolic resin incorporated with graphite powder and carbon

fibre was investigated.[3] The addition of CNT have significantly reduced porosity and increased interfacial interaction among phenolic-graphite composite. Moreover from the TGA analysis the thermal stability also increased by the addition of CNT to phenolic-graphite composite. Saghar et al.[38] have investigated the improvement in ablation properties of PF resin by the addition of MWCNT and silicon carbide. They found that the incorporation of MWCNT (upto 9%) has enhanced ablation properties.

In our previous work reduced Graphene oxide (RGO) was incorporated into the PF resin. Graphene oxide was reduced using green strategy (potato starch) and incorporated into PF matrix. The obtained nanocomposites exhibited exceptional improvement in mechanical and thermal properties.[39] Our group have also done large number of works in the field of PF macrocomposites.[40,41] In the present work, pristine MWCNT and MWCNT funtionalised with carboxyl groups were incorporated into phenol formaldehyde resin via in-situ polymerisation technique and compared the mechanical, thermal and morphological behaviour of the prepared nanocomposite. The carboxylated MWCNT were characterised by FT-IR, XRD, CHN analysis, X-ray photoelectron spectroscopy, AFM and Raman spectra. The mechanical, thermal and morphological analysis were conducted in order to compare the prepared nanocomposites. The morphological studies of the prepared nanocomposites were examined using scanning electron microscopy (SEM) and transmission electron microscopy (TEM). The thermal properties of the nanocomposites were analysed by thermogravimetric analysis (TGA) and differential thermal analysis (DTG).

Materials and methods

Materials

Phenol (99%), Formaldehyde solution (37%), Sodium hydroxide pellets (analytical grade) Glacial acetic acid (99–100%) were supplied by Merck, India for synthesis of resol resin. Multiwalled carbon nanotubes with an average diameter of 10–15 nm and average length 1–5 μm were supplied by ad-Nano Technologies Private Limited, India. The reagents used for carboxylation were sulfuric acid (H_2SO_4) (98%) and nitric acid (HNO_3) (69%).

Methods

Carboxylation of MWCNT. Carboxylation of MWCNT was done by adding concentrated H_2SO_4, and concentrated HNO_3 in (1:1) ratio. The reaction mixture is sonicated for one hour. The (1:1) reaction mixture is refluxed at 120 °C for 3 hours. After the reaction, the mixture was diluted with distilled water and allowed to sediment. The process repeated several times remove the acid and dried in the air oven. The powdered samples were taken for further analysis. Figure 1 shows schematic illustration of carboxylation of MWCNT.

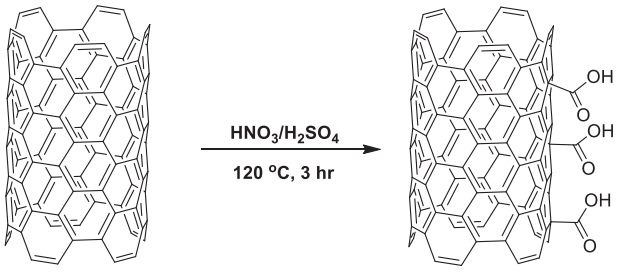

Figure 1. Schematic illustration of carboxylation of MWCNT.

Preparation of phenol formaldehyde resole resin-MWCNT/MWCNT-COOH nanocomposite. For the typical synthesis of resole resin F/P ratio =1.75:1 is taken. At first 0.5 mole% of sodium hydroxide solution is ultrasonicated with different loadings of MWCNT/MWCNT COOH (0.05, 0.08, 0.12, 0.15 wt%) for one hour. The resultant solution is refluxed with phenol at 95 °C for 15 minutes in a three neck round bottom flask. To this solution formaldehyde is slowly added within twenty minutes to ensure the polymerisation. The reaction is kept for 5–6 hours till it turns turbid. After the completion of reaction, the resin was allowed to cool and it was neutralised with glacial acetic acid to remove the water produced during condensation polymerisation. It was kept overnight and the aqueous layer was decanted off. The prepared nanocomposite was transferred to steel mould and subjected to step curing at different temperatures (60 °C for 2 hours, 70 °C for 12 hours, 80 °C for 3 hours, 90 °C, 100 °C, 110 °C for 1 hour and 120 °C for 4 hours). The resultant specimen was used for analysis.

Characterisations

Fourier transform infrared spectroscopy. Fourier Transform Infrared Spectroscopy was recorded using PERKIN ELMER ATR infrared spectrometer in the range of 400–4000 cm^{-1}. The FT-IR spectra were taken by making pellets of powdered samples (MWCNT, MWCNTCOOH) mixed with KBr.

X-ray diffraction analysis (XRD). The crystallinity and intensity changes of the samples (MWCNT, MWCNTCOOH) were recorded on Bruker AXS D8 Advance with Cu Kα radiation with an angle range 5°–80° (2θ angle range) at a wavelength of 1.541 Å, an operating voltage of 45 kV and a current of 35 mA.

CHN analysis. The percentage of carbon, nitrogen and hydrogen of MWCNT, MWCNTCOOH were analysed using CHN analyser (Elementar Vario EL III).

Thermogravimetric analysis. The thermal properties of the samples were analysed using Perkin Elmer, Diamond TG/DTG. About 10 mg of the prepared nanocomposites were put on the alumina cup and heated at a rate of 20 °C/min in Nitrogen atmosphere.

X-ray photoelectron spectroscopy. Samples were analyzed with XPS instrument TFA XPS from Physical Electronics (Münich, Germany). The samples were excited with monochromatic Al $K_{\alpha 1,2}$ radiation at 1486.6 eV.The analysis area was 400 μm^2. Emitted photoelectrons were detected with a hemispherical analyzer located at an angle of 45° with respect to the normal of the sample surface. Survey spectra were measured at a pass energy of 187 eV using an energy step of 0.4 eV. High-resolution spectra of C1s were measured at a pass energy of 29.35 eV using an energy step of 0.125 eV. An additional electron gun was used for surface charge neutralization during XPS measurements.

Atomic force microscopy (AFM). The surface morphology of pristine MWCNT and carboxylated MWCNT were characterised with Atomic Force Microscopy (WITec GmbH, Ulm, Germany) in contact mode at room temperature. The suspension of MWCNT and MWCNT-COOH was sonicated well and then analysed.

Raman spectrum. The Raman spectra of MWCNT and MWCNTCOOH were done using RA-Confocal Raman microscope with AFM (WITec GmbH, Ulm, Germany).

Scanning electron microscopy (SEM). The morphology of fracture samples were analyzed using JEOL Model JSM - 6390LV. To avoid charring the samples were sputtered with gold.

Transmission electron microscopy (TEM). The transmission electron micrographs of PF-MWCNT and PF-MWCNTCOOH nanocomposites.were obtained on a High-Resolution Transmission Electron Microscope, Jeol/JEM 2100. The ultramicrotome cutting was used to obtain TEM images of PF-MWCNT and PF-MWCNTCOOH nanocomposites.

Mechanical characterisation. The mechanical properties of the samples were tested using Universal Testing Machine (Tinius Olsen) according to ASTMD 638. The samples were cut into rectangular strips and the testings were conducted at room temperature with a gauge length of 60 mm and speed rate 2 mm/min.

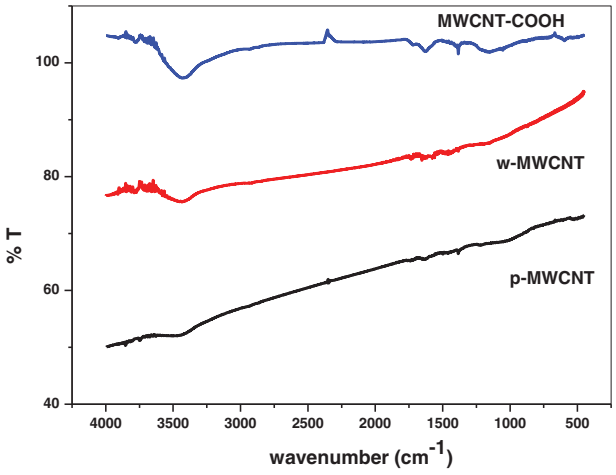

Figure 2. FT-IR analysis of pristine MWCNT, washed MWCNT and MWCNTCOOH.

Results and discussions

Characterisation of MWCNT; effect of modification

FT-IR characterisation. Figure 2 shows the FT-IR spectra of pristine MWCNT (p-MWCNT), washed MWCNT (w-MWCNT), and carboxylated MWCNT (MWCNT-COOH).The broad peak around 3500 cm^{-1} is due to the presence of hydroxyl group along the the side walls of multiwalled carbon nanotubes. This peak is not present in p-CNT indicates the successful funtionalisation of MWCNT. But for w-MWCNT a less intense peak at 3500 cm^{-1} is present because MWCNT have a tendency for air oxidation. The hydroxyl groups can be from atmospheric moisture. But for carboxylated MWCNT the intensity of hydroxyl group is much higher. Similar results were obtained for other researchers.[42,43] The small peak at 1720 cm^{-1} was assigned for carbonyl stretching vibrations. The CNT-COOH showed peak at 1640 and 1175 cm^{-1} which is characteristic peak of C = O and C-O respectively. The peak at 1400 cm^{-1} was attributed to the bending vibration of hydroxyl groups attached on the side walls of MWCNT.[44] These results showed the successful funtionalisation of MWCNT. The small peak at 600 cm^{-1} is due to the presence of –C-O-C- groups. The results obtained were in accordance with previous reports.[45–47] The importance of funtionalisation of CNT helps on anchoring with polymer or other moieties.

CHN analysis of p-MWCNT and MWCNTCOOH. CHN analysis gives elemental composition of light elements such as carbon, nitrogen and hydrogen. There is relative decrease in the carbon content in the oxidised MWCNT (Table 1). The hydrogen content slightly increases and nitrogen content slightly decreases. These results summarises the formation of defects on

the surface of MWCNT which in turn helps the attachment of carboxyl groups on the surface. This results are in accordance with FT-IR spectrum. Trace amount of nitrogen was detected in pristine MWCNT due to nitrogen gas absorbed during the preparation of MWCNT (MWCNT procured was prepared using chemical vapour deposition in the presence of nitrogen gas).[48,49] Small level of sulphur may be due to presence of acidic mixture even after several washing.

XRD analysis. All the two specimen shows two major diffraction peak at $2\theta = 25.68$ and 42.53 which implies (002) and (100) planes respectively. The two theta at 53.53° is the diffraction of (004) reflection planes.[50] These reflection planes are due the adjacent graphitic layers. Additional peaks at 44.9 and 56.5 can be attributed to (101) and 102 reflection planes. From the XRD studies it is clear that there is small change in the intensity of pure MWCNT and modified MWCNT. The difference in intensity is due to the generation of some defects on the sidewalls of MWCNT. The intensity variations can be attributed to the lattice distortions as a result of surface treatments. Carboxylation reduces the bundling of MWCNT and thereby changing the diffraction patterns. As a result the crystalline size decreases and the peaks got weakened and broadend in accordance with previous reports.[51] All these results attributed to the attachment of functional groups on the side walls of MWCNT. Figure 3 shows the XRD spectrum of p- MWCNT, MWCNT-COOH.

Raman spectrum. Further evidence for carboxylation of MWCNT was obtained from Raman spectra analysis (Figure 4). The importance of Raman spectroscopy relies on the efficiency to characterize the crystal structure of carbonaceous material. The D band represents the defective sites in sp^2 hybridised carbon systems while G band gives idea about vibrational modes of graphitic carbon, G' is the second order raman scattering process which indicates the crystallinity of the carbonaceous material. The change in intensity of D band reveals the increasing defects on the side walls or the ID/IG ratio for p-MWCNT is also ~1.01. The ratio of relative intensity of the peak gives an idea about the defects generated during modifications. ID/IG ratio for MWCNT-COOH is ~0.86 which can be attributed to the generation of defective sites. The decrease in ID/IG ratio may be due to the removal of some amorphous carbon.[52] These ratios show the degree of funtionalisation. Too much variation in ID/IG shows the disruption of graphitic structure. Fashedemi et al.[53] modified MWCNT with carboxyl groups and got similar results. These results clearly show that funtionalisation does not disrupt the aromatic system prominently.

Table 1. CHN Analysis of p-MWCNT and MWCNTCOOH.

Sample no.	Sample name	N%	C%	S%	H%
1	CNT(P)	1.07	95.52	ND	ND
2	CNTCOOH	0.92	61.49	0.74	0.18

ND: not detected.

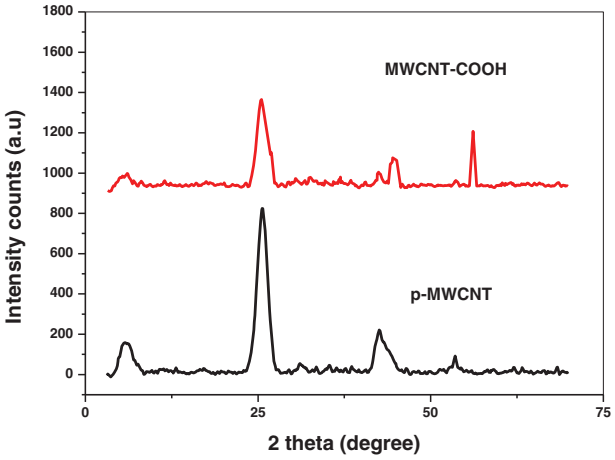

Figure 3. XRD spectrum of p- MWCNT, MWCNT-COOH.

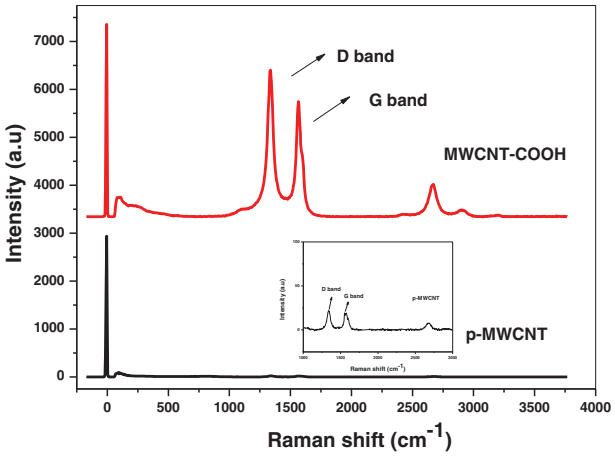

Figure 4. Raman Spectra- p-MWCNT, MWCNT-COOH.

X-ray photoelectron spectroscopy. XPS is a powerful technique used to find the functional groups attached on the surface of a material. The binding energy of CNT when irradiated with X-rays determines its surface composition. Pristine MWCNT showed a C1s peak at 284.4 eV (Figure 5) which attributes to the graphitic structure.[54] In the case of carboxylated MWCNT another peak at 289 eV (Figure 6) is appeared which shows the attachment of COOH groups on the sidewalls of MWCNT.[55] The π- π^* transition peak was observed at 289 eV which corresponds to attachment

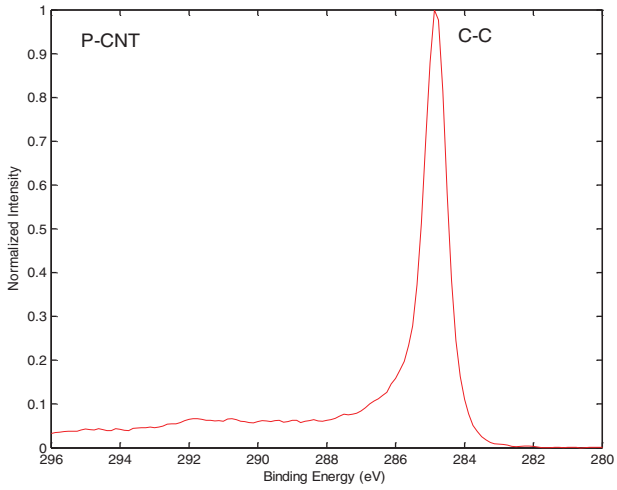

Figure 5. High-resolution XPS peak of carbon C1s for p-MWCNT.

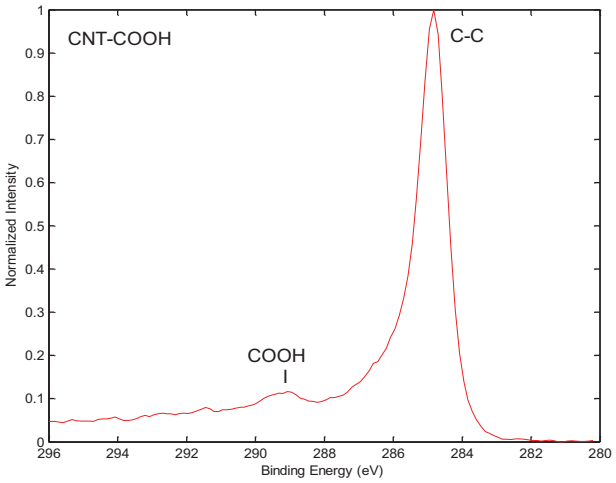

Figure 6. High-resolution XPS peak of carbon C1s MWCNT-COOH sample.

of oxygen moieties. The major peak (284.4 eV) found in pristine MWCNT and MWCNT COOH were similar.

Atomic force microscopy (AFM). The surface topography of p-MWCNT and MWCNT COOH was shown in Figures 7 and 8 The AFM image of pristine MWCNT is well separated but carboxylated MWCNT is not uniformly spread out well. The average thickness of pristine MWCNT and carboxylated MWCNT observed was 1.27 nm and 8.53 nm respectively. The average surface roughness of pristine MWCNT and carboxylated MWCNT was 2.81 nm and 15.21 nm.

Mechanical properties of PF-MWCNT and PF-MWCNTCOOH

The factors affecting the mechanical properties of the nanocomposites are filler dispersion, geometry of the filler, interfacial bonding and aspect ratio. Agglomeration of the filler results in the reduction of aspect ratio of the filler thereby decreasing the mechanical properties of the prepared nanocomposites. The effective load transfer is possible only if there exists strong interfacial interaction between the polymer matrix and nanofiller. The addition of carbon nanotubes will definitely improve the mechanical properties of the nanocomposite.[56]

Stress-strain behaviour. The tensile strength, modulus, elongation, stress-strain showed a maxima for 0.12 wt% and 0.08 wt% for PF-MWCNT and PF-MWCNTCOOH nanocomposite respectively. This can be attributed to the increased interaction between MWCNT/MWCNTCOOH with phenolic matrix

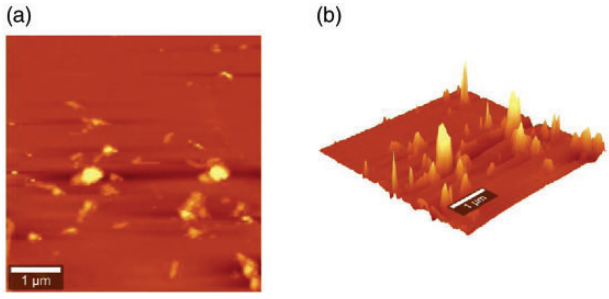

Figure 7. AFM of p-CNT: (a) 2 D image (b) 3 D image.

compared to filler-filler interaction. Very good dispersion of nanofillers helps to improve efficient load transfer. The stress-strain behaviour of the prepared nanocomposite is shown in Figure 9(a). The ultimate stress expresses the maximum load a sample can afford before it breaks. MWCNT and MWCNTCOOH improved the plasticizing effect of the nanocomposite. The formation of interconnecting network of nanofillers inside the PF matrix retards the easy breakage of the composite upon an external stress. The neat PF showed a brittle nature. The incorporation of both MWCNT and MWCNTCOOH has decreased the inherent brittleness. The addition of nanofillers brought more hard and tough nature to the nanocomposite. At first the nanocomposite showed a linear behaviour and thereafter observed non linearity till the complete failure of the nanocomposite. For PF-MWCNT, 0.12 wt% expressed maximum load transfer. Higher loading of the MWCNT (0.15 wt%) increased stress centres due the agglomeration of the MWCNT. The aggregation of MWCNT restricted the effective load transfer between the matrix and the nanofiller.

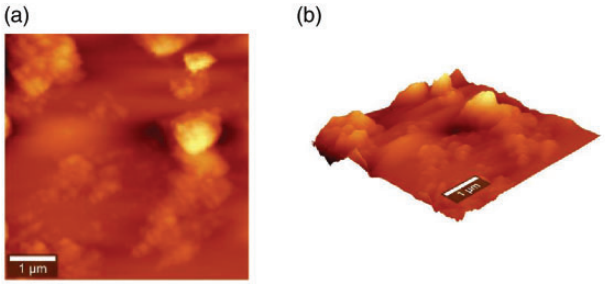

Figure 8. AFM of CNT-COOH: (a) 2 D image (b) 3 D image.

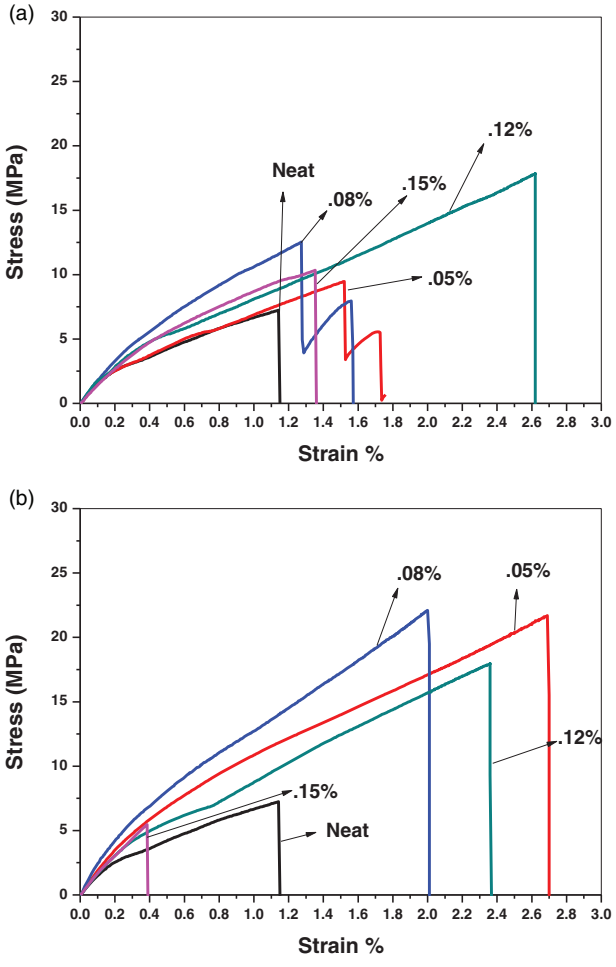

Figure 9. (a) Stress-Strain of PF-MWCNT and (b) PF-MWCNTCOOH nanocomposites.

Like any other properties, mechanical properties also have a percolation, beyond that critical point further addition of nanofillers will not improve the properties.[57] At lower loading a homogenius dispersion of MWCNT is expected which resulted in enhancement of mechanical properties. For PF-MWCNTCOOH, 0.08 wt% exhibited maximum load transfer. 0.12 wt% and 0.05 wt% MWCNT COOH loading improved the toughness of the nanocomposite but the stress value is reduced. In the case of PF-MWCNTCOOH, 0.15 wt% filler loading decreased the value of stress and the prepared nanocomposite showed more ductility (Figure 9 (b)). This can be attributed to the agglomeration of the nanofillers which blocks the effective load transfer between the filler and polymer matrix. The decrease in strain at higher filler loadings are due restricted mobility of polymer chains by large number of nanotubes. This will leads to brittleness of the nanocomposite. The addition of both MWCNT and MWCNTCOOH did not change the failure pattern of the nanocomposite further it enhanced the stiffness of the specimen.

Tensile behaviour. The tensile strength of PF-MWCNT composites increased by 6.32% when the filler loading is 0.05 wt%. For 0.08 wt% the increase is 68.4% and for 0.12 wt% is 115.2% and for 0.15 wt % is 26.6% (Figure 10). The tensile strength of PF-MWCNTCOOH composites increased by 169% when the filler loading is 0.05 wt%. For 0.08 wt% the increase is 185% and for 0.12 wt% is 90%. However, for PF-MWCNTCOOH composites with 0.15 wt %, the tensile strength decreased upto 32%. For 0.15 wt %, agglomeration resulted in property reduction due to the poor dispersion and interface interaction. At higher wt% the effective aspect ratio is reduced due to the entaglement of MWCNT. This results were in accordance with Wu et al.[58] They have compared the properties of phenol formaldehyde by reinforcing graphene nanosheets and carbon nanotubes in various filler loadings. Addition of carbon nanotubes improved the tensile strength and young's modulus. Their tensile strength was improved only up to 54.7% by the addition of 0.6 wt% of carbon nanotubes. Bridging between the nanofiller and the polymer plays a crucial role in improving the mechanical properties of the nanocomposite. It is expected that the funtionalisation of MWCNT decreases the diameter and can bridge the crack interface thereby enhancing the mechanical properties.[59]

Young's modulus. Due to the high aspect ratio and high surface CNT serves as a perfect candidate for improving the mechanical properties of a polymer. The funtionalised CNT improve the mechanical properties since it brings good dispersion and efficient stress transfer. Analysing the results we found that at higher wt%, (0.15 wt%) the mechanical properties decreases. We suggest that this phenomenon is due to the aggregation of Multiwalled Carbon nanotubes. The non homogenius dispersion of MWCNT would leads to bad

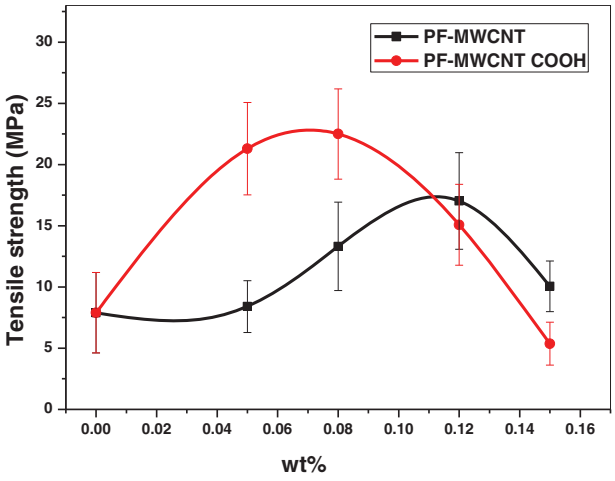

Figure 10. Tensile properties of (a) PF-MWCNT and (b) PF-MWCNTCOOH nanocomposites.

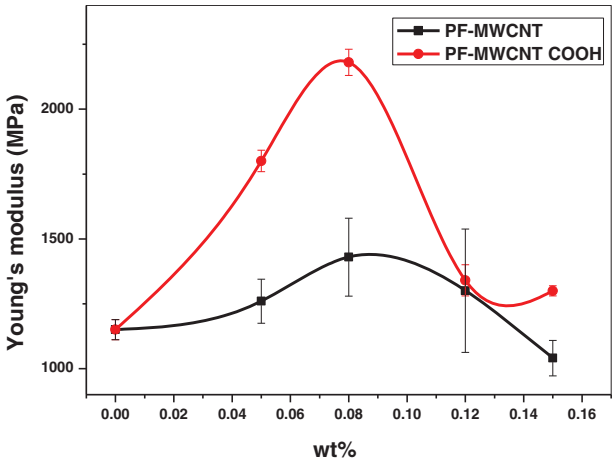

Figure 11. Young's modulus of (a) PF-MWCNT and (b) PF-MWCNTCOOH nanocomposites.

interaction with the PF matrix and restricting the dissipation of energy during the fracture process. During the fracture process, homogenius dispersion of the MWCNT in PF matrix could lead to an increase in energy dissipation. In the case of Young's modulus, the same trend was observed (Figure 11). For 0.05 wt%, 0.08 wt%, and 0.12 wt% the young's modulus increased by 9.6%, 25.34%, 13.1% respectively compared to neat. For 0.15 wt% the Young's modulus decreased up to 9.6% due to development of stress points at as a result of agglomeration of MWCNT. The increase in the mechanical properties can be attributed to the effective load transfer between the filler and the host matrix.

In the case of PF-MWCNTCOOH, for 0.05 wt%, 0.08 wt%, 0.12 wt% and 0.15 wt% the Young's modulus increased by 56.5%, 89.5%, 16.52% and 13.04% respectively compared to neat. The improvement in mechanical properties is due the good interfacial interaction between the MWCNT and PF matrix. The carboxyl groups of MWCNT interact well with –OH, ether, methylene groups present in the PF matrix and makes an effective network. This brings better stress transfer between filler and the matrix. The extent of load transfer is the key factor which determines the mechanical properties of the synthesized nanocomposite. It is well-known that the lack of energy dissipation during crack propagation will eventually lead to brittleness of the prepared nanocomposite. Here MWCNT COOH dissipates energy better than MWCNT because the carboxyl groups interact well with functional groups of PF matrix.

Elongation at break. The elongation at break of the prepared nanocomposite is shown in Figure 12. The maximum elongation is observed for 0.12 wt% and 0.08 wt% for PF-MWCNT and PF-MWCNTCOOH nanocomposite respectively. The incorporation of MWCNT and MWCNT-COOH enhanced the mobility of PF resin thereby increasing the flexibility of the prepared nanocomposite. The better interfacial compatibility of MWCNT and MWCNT-COOH with the PF matrix is the reason for this increment. Similar results were observed for other authors.[60–62]

Thermal analysis

Thermogravimetry analysis (TGA) and derivative thermo-gravimetric analysis (DTG) of MWCNTCOOH

The thermal properties of the prepared PF-MWCNT nanocomposite were studied by TGA and DTG (Figure 13(a) and (b)). It is clear from the result that the thermal stability of PF-MWCNT nanocomposite increased with increasing content of MWCNT. There are two stages of degradation *viz* first stage from 0–350°C and second stage from 350–700°C. During the first stage absorbed water is released. In the second stage is attributed to the degradation of existing oxygen containing groups, and methylene-benzene bonds. Here MWCNT loading increased the thermal stability than neat. MWCNT shows higher thermal stability and temperature resistant. The peak points observed in DTG curves also increases with increasing filler loadings and is summarised in Table 2.

The thermal degradation properties of the prepared PF-MWCNT COOH was analysed by TGA and DTG. It is observed that the incorporation of carboxylated MWCNT into the resin improved the thermal stability (Figure 14(a) and (b)) of the prepared nanocomposite.

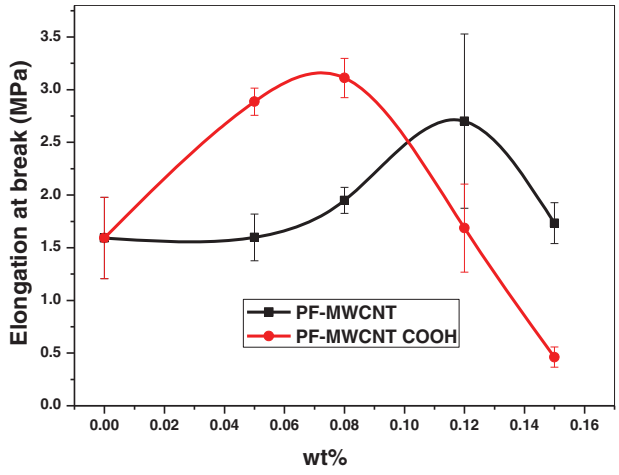

Figure 12. Elongation at break of (a) PF-MWCNT and (b) PF-MWCNTCOOH nanocomposites.

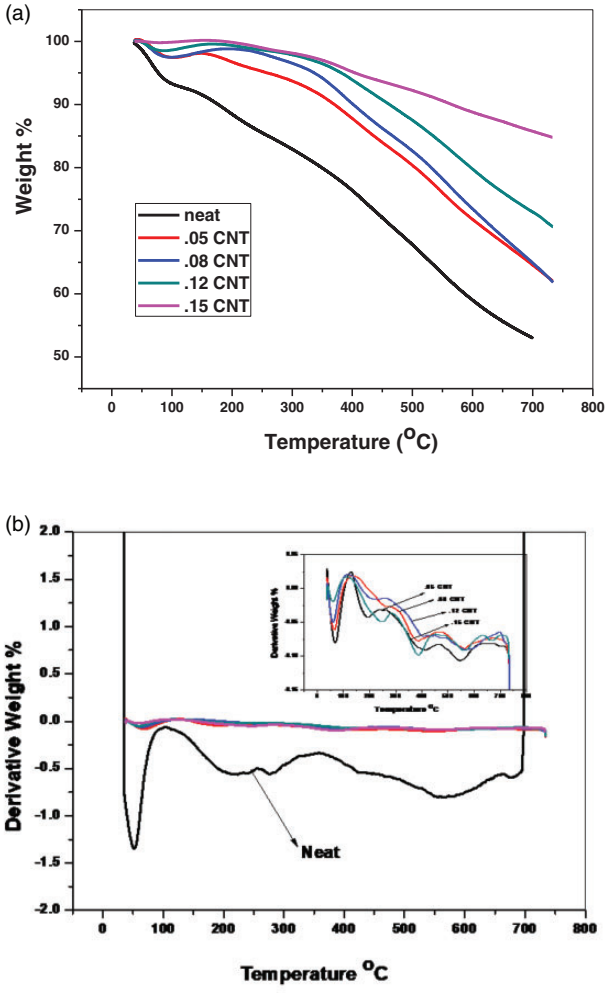

Figure 13. (a) TGA of PF-MWCNT nanocomposite (b) DTG of PF-MWCNT nanocomposite.

Table 2. TGA/DTG profile of PF-MWCNT nanocomposite.

Sample	At 350 oC(wt%)	Char Yield At 700 oC (wt%)	DTG peak point
Neat	79.9	53.5	66.85
.05	91.33	64.53	545.96
.08	91.18	64.90	561.44
.12	96.45	72.95	562.96
.15	97.01	85.74	562.02

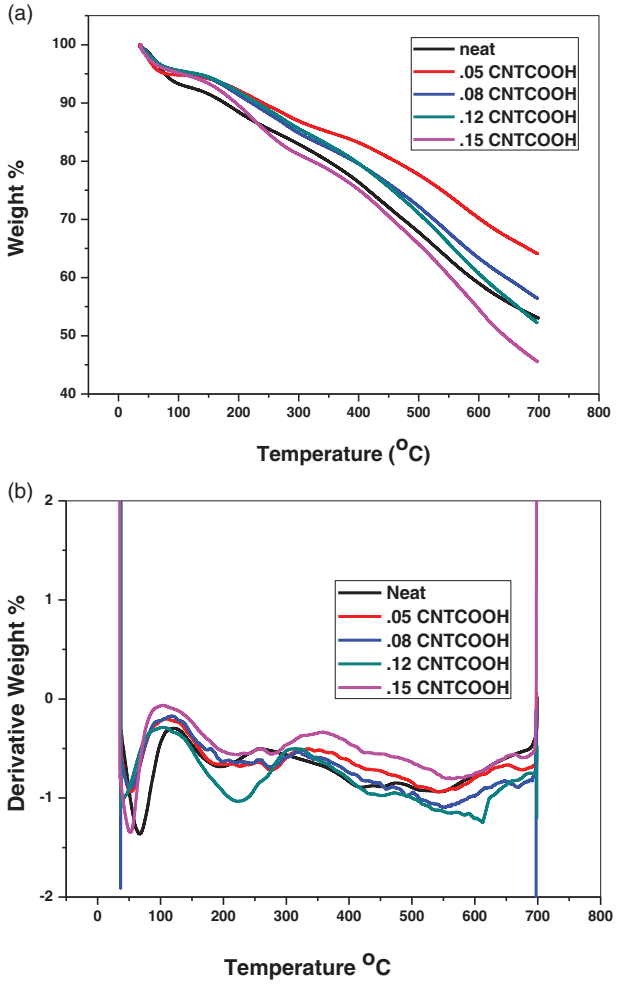

Figure 14. (a) TGA of PF-MWCNT-COOH nanocomposite (b) DTG of PF-MWCNT-COOH nanocomposite.

But compared to pristine MWCNT nanocomposite, the degradation rate was higher. This is due to rapid degradation of phenolic resin by the addition of carboxylated MWCNT. The faster degradation rate is due to the presence of functional groups on the surface of MWCNT.[63] The decomposition temperature between 150 °C–350 °C is mainly due to the carboxyl groups present.[64] The better interaction of phenol

formaldehyde and MWCNTCOOH resulted in faster degradation as compared to MWCNT reinforced PF nanocomposite due to the presence of these carboxyl groups. The defective sites generated by the attachment of carboxyl and hydroxyl groups is the reason for less thermal stability compared to pristine MWCNT.[65] MWCNTCOOH have a tendency to increase heat of diffusion, it increases the thermal conductivity, thermal diffusivity of the nanocomposite thereby decreasing the thermal stability.[66–68] The addition MWCNT COOH enhanced the thermal stability upto 0.12 wt% and decreased for 0.15 wt%. The char yield of 0.05 wt% and 0.08 wt% increased compared to the neat resin. As we observed in TGA of MWCNT-COOH, the thermal stability decreased as compared to pure MWCNT due to the presence of defective sites on the sidewalls of the nanotubes. This is the reason for decrease in thermal stability at higher filler loadings (0.12 wt% and 0.15 wt%). At lower concentration of MWCNT-COOH it shows much better thermal stability than the neat. Figure 14 represents TGA and DTG of PF-MWCNT COOH nanocomposite respectively. Table 3 summarises TGA/DTG profiles of PF-MWCNTCOOH.

Table 3. TGA/DTG profile of PF-MWCNTCOOH nanocomposite

Sample	At 350°C (wt%)	Char Yield At 700 °C (wt%)	DTG peak point
Neat	79.9	53.5	66.85
.05	85.1	64.3	53.61
.08	82.2	56.4	55.14
.12	82.1	52.3	54.86
.15	78.5	45.5	53.6

Surface morphological analysis of PF-MWCNT and PF-MWCNT COOH nanocomposite

Scanning electron microscopy (SEM)

The surface morphology of the fracture surface after tensile tests of pure PF, and PF nanocomposites were revealed by SEM photographs (Figure 15). SEM images show filler-matrix interaction and fracture behaviour of the nanocomposite. Inorder to compare the fracture behaviour of different filler loadings, these are observed at same magnification. Here the neat resin exhibited highly brittle nature, which attributes to the higher crack initiation due to less fracture toughness (Figure 15(a)). Neat PF showed smooth brittle surface due to less resistance to crack propagation. The incorporation of pure MWCNT and MWCNT COOH has totally changed the fracture surface. The addition of pure MWCNT and MWCNT COOH increased the fracture toughness by making deformation in the plastic.[69] The capability of absorbing energy is defined as fracture toughness. During the fracture process small cracks are developed. In the case of neat matrix there is increase in crack propagation thereby decreasing the fracture toughness. Higher energy is absorbed for fracture process in the case of MWCNT/MWCNT COOH reinforced matrix so the fracture mode differs. This will lead increase in fracture toughness. Compared to pure MWCNT reinforcement, MWCNT COOH shows better fracture toughness. Schematic representation of crack progation is shown in Figure 16. Carboxylation of MWCNT improved interaction with PF matrix than pristine MWCNT. Studies showes that cylindrical particles with less diameter can interact more with polymer matrix.[56,70] As the interfacial adhesion increases better load transfer is observed which eventually leads to improvement in fracture toughness. The strong interfacial interaction of MWCNT COOH with PF matrix improved mechanical properties and resistance towards crack. Effective load transfer ensures the better functioning of composite materials. Better fracture toughness depends on the effective load transfer between nanofiller and polymer matrix and also higher interfacial adhesion between these two. Here MWCNT COOH shows better fracture toughness since it interacts with functional groups of PF matrix than MWCNT.

Transmission electron microscope (TEM)

Figure 17 shows the TEM images of 0.12 wt% PF-MWCNT and 0.08 wt% PF-MWCNTCOOH. TEM is powerful technique which provides a qualitative information about the interaction between nanofillers and the polymer matrix. Since MWCNT is composed of carbon atoms it blocks the transmission of light from the light source of optical microscope. In case of phenolic resin reinforced with pristine MWCNT, it forms some aggregates. This evident from dark spots observed on the image. This is due to the agglomeration of pure MWCNT. But when the carboxylated MWCNT was reinforced it dispersed well inside the PF matrix. The surface functional groups present in MWCNT interact well with PF matrix. The presence of carboxyl groups on the surface of MWCNT reduced agglomeration inside the matrix which can be well observed from the TEM image.

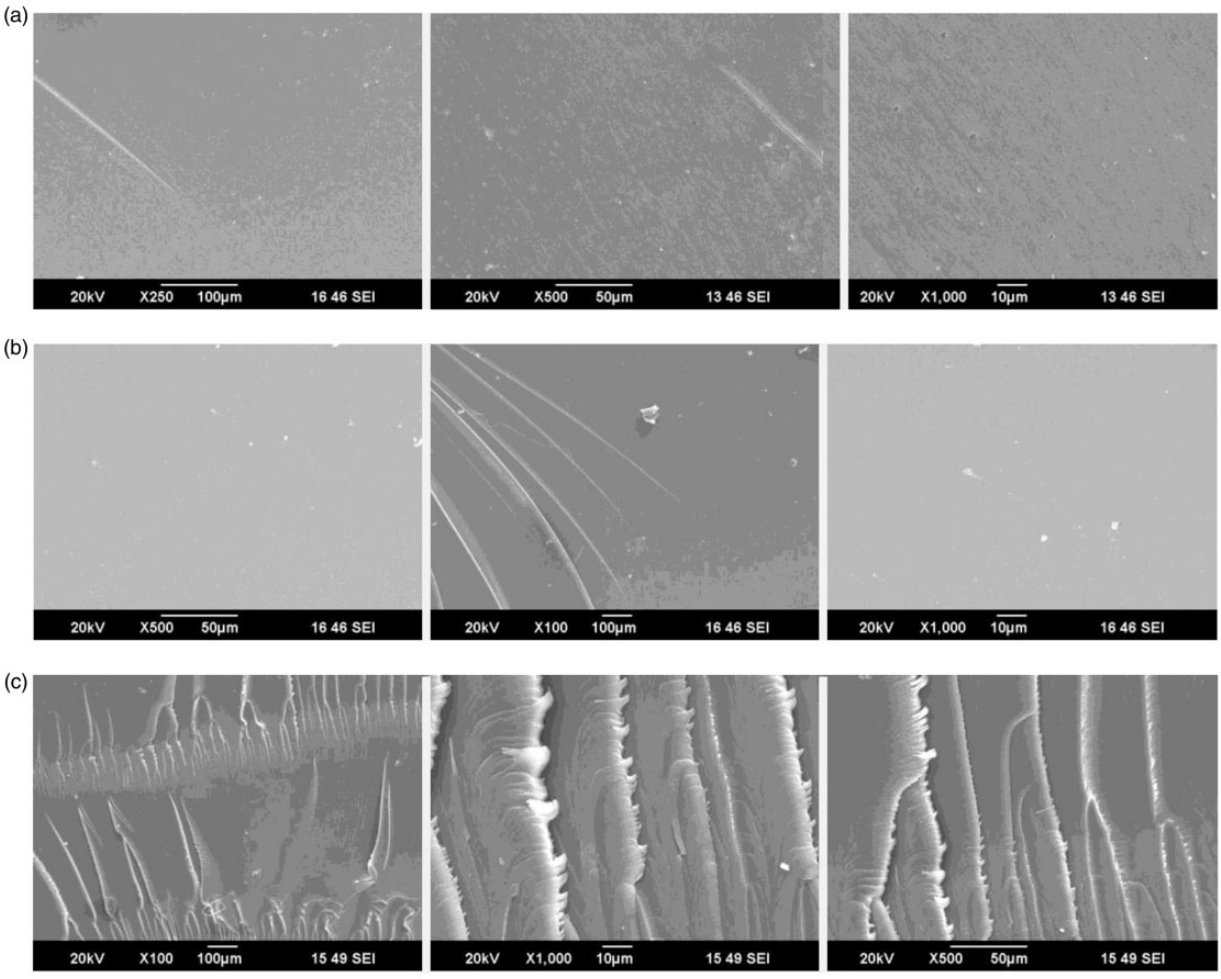

Figure 15. Fracture surface of (a) neat (b) 0.12 wt% PF-MWCNT (c) 0.08 wt% PF-MWCNTCOOH.

Theoretical modelling of Young's modulus

Several theoretical models have been proposed in order to understand the mechanism of reinforcement in nanocomposites. Among them Halpin-Tsai model is widely used for theoretical modelling of fibres as well as sheet or platelet like nanofillers. The Halpin-Tsai equation used for randomly oriented fibres reinforced polymer matrix is given below.[71,72]

$$\frac{E_{Random}}{E_m} = \frac{3}{8}\left[\frac{1+2(l_f/d_f)n_L V_f}{1-n_L V_f}\right] + \frac{5}{8}\left[\frac{1+2n_T V_f}{1-n_T V_f}\right] \quad (1)$$

$$n_L = \frac{\frac{E_f}{E_m}-1}{\frac{E_f}{E_m}+2(l_f/d_f)} \quad (2)$$

$$n_T = \frac{\frac{E_f}{E_m}-1}{\frac{E_f}{E_m}+2} \quad (3)$$

where E_{Random}, E_f, E_m are the effective modulus of nanocomposite, MWCNT and polymer matrix respectively.

l_f, d_f are length and diameter of MWCNT respectively.

V_f is the volume fraction of MWCNT.

The effective modulus of the MWCNT was calculated by assuming that the outer wall holds the entire load form the polymer matrix by using the expression,

$$E_f = \frac{4t}{d} E_{CNT} \quad (4)$$

Where t is the thickness of outer wall of MWCNT and d is the diameter of MWCNT, the effective modulus of for MWCNT was 1 TPa[73] and the effective

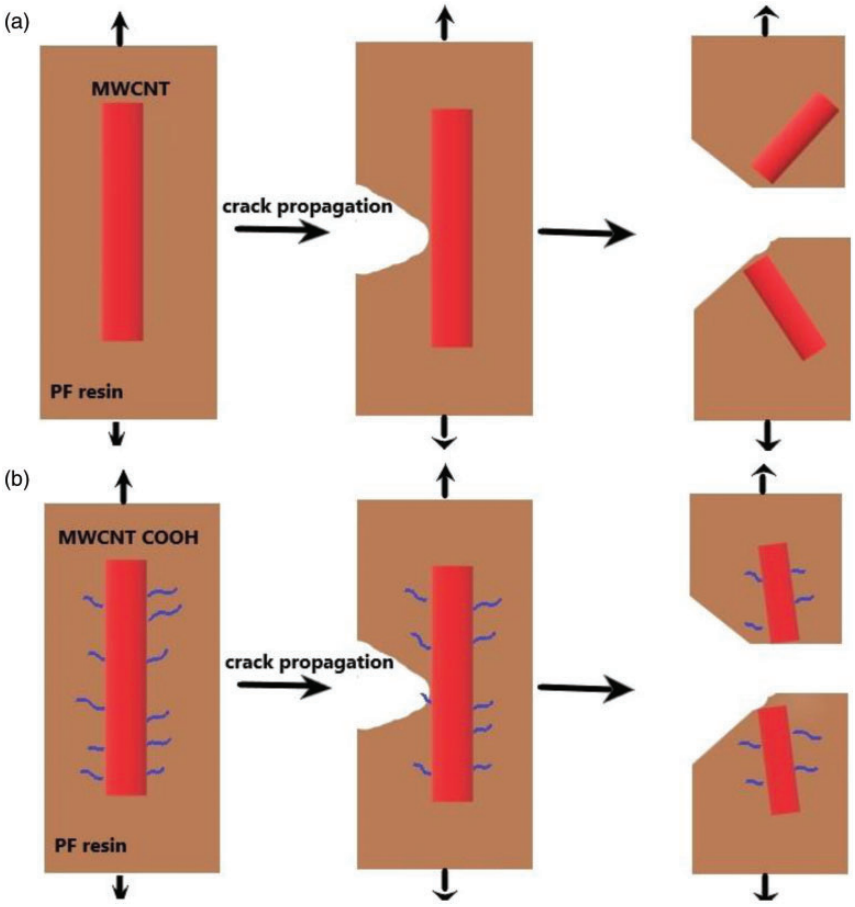

Figure 16. Schematic representation of possible crack propagation of (a) PF-MWCNT (b) PF-MWCNTCOOH.

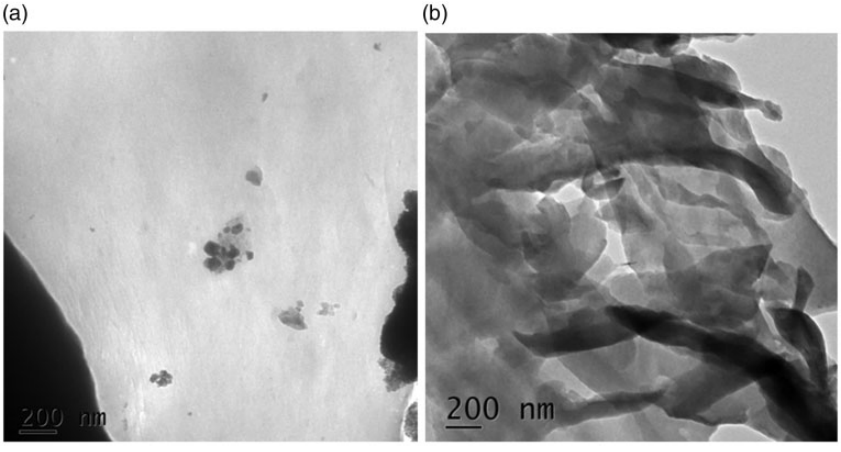

Figure 17. TEM image of (a) PF-MWCNT (0.12 wt%) (b) PF-MWCNTCOOH (0.08 wt%).

modulus of nanocomposite obtained was 1.59 GPa. The Young's modulus obtained from tensile tests of PF-MWCNT and PF-MWCNT COOH are adopted as effective modulus (E_m) for using in Halpin Tsai modelling. Here we plotted tensile modulus versus volume fraction of nanofiller (MWCNT and MWCNT COOH) and found that lower filler loading moderately fits with The experimentally obtained values for tensile modulus found good agreement with theoretical values for both reinforcements

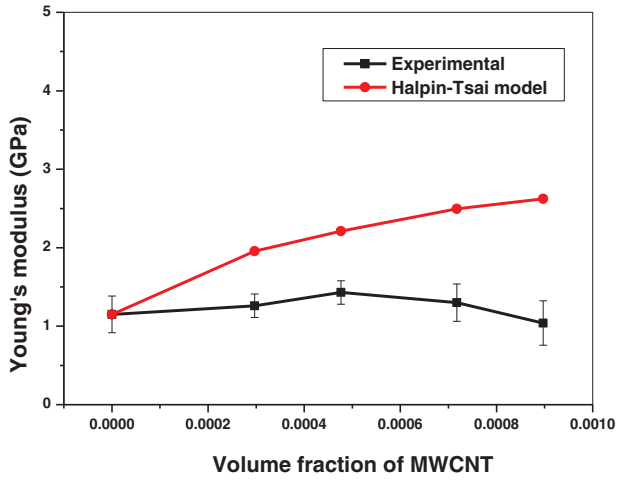

Figure 18. Comparison of theoretical and experimental values PF-MWCNT.

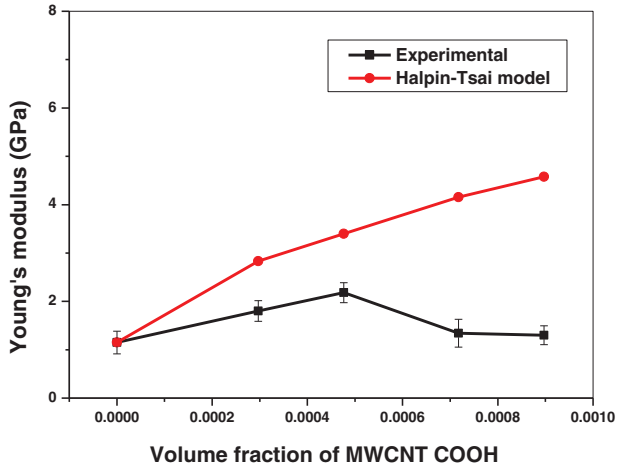

Figure 19. Comparison of theoretical and experimental values PF-MWCNT COOH.

(Figures 18 and 19) In the case of PF matrix reinforced with pristine MWCNT (Figure 18) experimental results illustrates the addition of MWCNT increased the Young's modulus from 0 wt% to 0.12 wt% and then decreases. The percentage error between experimental and theoretical values of tensile modulus for 0.05 wt%, 0.08 wt%, 0.12 wt% and 0.15 wt% are 36%, 35%, 48%, and 60%, respectively.

For PF matrix reinforced with MWCNT COOH (Figure 19) experimental results showed the addition of MWCNT COOH increased the Young's modulus from 0 wt% to 0.08 wt% and then decreases. The percentage error between experimental and theoretical values of tensile modulus for 0.05 wt%, 0.08 wt%, 0.12 wt% and 0.15 wt% are 36%, 37%, 68%, and 72% respectively. Larger deviation at higher filler loading may be due to agglomeration by van der Waals force of attraction among the nanotubes.[74] From the results it is assumed that MWCNT are homogeniusly dispersed in PF matrix and it showed better interfacial interaction.

Conclusions

Phenolic resins are excellent synthetic polymers used from early times due to its excellent properties like ease of moulding, good dimensional stability, chemical and weather resistance, electrical insulation, and low water uptake. The incorporation of nanofillers enhances the properties of PF resin. The present work deals with the incorporation of pure MWCNT/MWCNTCOOH into the PF matrix. The characterization of funtionalised MWCNT was done by XRD, FT-IR, CHN analysis, XPS analysis, AFM and Raman spectra. The results confirmed the surface modification of MWCNT with carboxyl groups.

It is well established that the enhancement of properties of polymer nanocomposites depends on properties such as the dispersion state, filler geometry, and filler–filler interaction. Good dispersion of MWCNT/MWCNT COOH in the PF matrix can promote the effective load transfer which brings about the improvement in the mechanical properties. Lower filler loading increased the mechanical properties ie, upto 0.12 wt%. At higher loading (.15 wt%) due to ineffective stress transfer the mechanical properties decreased. In the case of PF-MWCNTCOOH 0.08 wt% showed higher mechanical properties. The agglomeration of MWCNT COOH at higher concentration will lead to the formation of stress centres at certain points. Therefore we can conclude very minimal amount of MWCNT/MWCNT COOH can enormously increase the mechanical properties of the prepared nanocomposites. The Thermal analysis of PF nanocomposite showed increased thermal stability. Compared to neat PF composite MWCNT addition improved the thermal stability. The addition of 0.15 wt% improved the char yield by 60%. The incorporation of carboxylated MWCNT enhanced the thermal stability of the prepared PF nanocomposite but was less compared to MWCNT reinforcement. The morphological analysis (SEM, TEM) of the prepared nanocomposite reveals that incorporation of the filler increased fracture toughness and better dispersion. The experimentally obtained values for tensile modulus found good agreement with theoretical values for both MWCNT and MWCNT COOH reinforcements.

Highlights

- Two types of Phenol-formaldehyde nanocomposites were prepared using pure MWCNT(p-MWCNT) and carboxylated MWCNT(MWCNTCOOH).
- MWCNT was modified with carboxyl groups and was confirmed by XRD, FT-IR CHN analysis, Atomic force microscopy, X-ray photoelectron spectroscopy and Raman spectra
- Compared to p-MWCNT, MWCNTCOOH reinforcement improved the mechanical properties of the PF nanocomposites. The maximum load transfer for PF-MWCNT and PF-MWCNTCOOH nanocomposites were exhibited by 0.12 wt% and 0.08 wt% reinforcement respectively.
- MWCNT COOH shows better fracture toughness compared to pure MWCNT reinforcement.
- TEM analysis showed better dispersion of MWCNT after carboxylation than pristine MWCNT
- Halpin-Tsai modelling showed good agreement with experimental values of tensile modulus.

Declaration of Conflicting Interests

The author(s) declared no potential conflicts of interest with respect to the research, authorship, and/or publication of this article.

ORCID iD

MS Sreekala https://orcid.org/0000-0002-9357-0947

Funding

The author(s) disclosed receipt of the following financial support for the research, authorship, and/or publication of this article:The authors are grateful to the financial support from KSCSTE Thiruvananthapuram, Kerala, under SRS scheme, DST, New Delhi for the facilities provided to Sree Sankara College, Kalady under DST-FIST programme (No. 487/DST/FIST/15-16).

References

1. Peng B, Jiang Y and Zhu A. A novel modi fi cation of carbon nanotubes for improving the electrical and mechanical properties of polyethylene composites. *Polym Test* 2019; 74: 72–76.
2. Vajaiac E, Palade S, Pantazi A, et al. Mechanical properties of multiwall carbon nanotube-epoxy composites. *Dig J Nanomater Biostructures* 2015; 10: 359–369.
3. Nguyen TH, Vu MT, Le VT, et al. Effect of carbon nanotubes on the microstructure and thermal property of phenolic/graphite composite. *Int J Chem Eng* 2018; 2018: 1–8.
4. Endo M, Takeuchi K, Igarashi S, et al. The production and structure of pyrolytic carbon nanotubes (PCNTs). *J Phys Chem Solids* 1993; 54: 1841–1848.
5. Iijima S. Helical microtubules of graphitic carbon. *Nature* 1991; 354: 56–58.
6. Chaudhury S and Sinha SK. *Carbon nanotube and nanowires for future semiconductor devices applications*. Amsterdam: Elsevier Inc., 2019.
7. Liu Y, Ma Z, Wang S, et al. Carbon nanotube-based photovoltaic receiver with open-circuit voltage larger than 10 V. *Nano Energy* 2019; 57: 241–247.
8. Barzola-Quiquia J, Esquinazi P, Lindel M, et al. Magnetic order and superconductivity observed in bundles of double-wall carbon nanotubes. *Carbon N. Y* 2015; 88: 16–25.
9. N'Diaye J and Lian K. Polymerized Fuchsin and modified carbon nanotube electrodes for electrochemical capacitors. *Nano-Structures Nano-Objects* 2018; 15: 173–179.
10. Hassanzadeh-Aghdam MK and Ansar R. Thermal conductivity of shape memory polymer nanocomposites containing carbon nanotubes: A micromechanical approach. *Compos Part B Eng* 2019; 162: 167–177.
11. Mai H, Mutlu R, Tawk C, et al. Ultra-stretchable MWCNT–ecoflex piezoresistive sensors for human motion detection applications. *Compos Sci Technol* 2019; 173: 118–124.
12. Natsuki T, Tantrakarn K and Endo M. Prediction of elastic properties for single-walled carbon nanotubes. *Carbon N Y* 2004; 42: 39–45.
13. Zare Y and Rhee KY. Simplification and development of McLachlan model for electrical conductivity of polymer carbon nanotubes nanocomposites assuming the networking of interphase regions. *Compos Part B Eng* 2019; 156: 64–71.
14. Kaymakci A, Birinci E and Ayrilmis N. Surface characteristics of wood polypropylene nanocomposites reinforced with multi-walled carbon nanotubes. *Compos Part B Eng* 2019; 157: 43–46.
15. Sumdani MG, Islam MR, Yahaya ANA, et al. Acid-Based Surfactant-Aided Dispersion of Multi-Walled Carbon Nanotubes in Epoxy-Based Nanocomposites. *Polym Eng Sci* 2018; 59: E80–E87. DOI: 10.1002/pen.24966.
16. Hirano K and Asami M. Phenolic resins-100 years of progress and their future. *React Funct Polym* 2013; 73: 256–269.
17. Mougel C, Garnier T, Cassagnau P, et al. Phenolic foams: a review of mechanical properties, fire resistance and new trends in phenol substitution. *Polymer (Guildf)* 2019; 164: 86–117.
18. Crespy D, Bozonnet M and Meier M. 100 Years of bakelite, the material of a 1000 uses. *Angew Chem Int Ed* 2008; 47: 3322–3328.
19. Zhang R, Jin X, Wen X, et al. Alumina nanoparticle modified phenol-formaldehyde resin as a wood adhesive. *Int J Adhes Adhes* 2018; 81: 79–82.
20. Shahi S, Roghani-Mamaqani H, Salami-Kalajahi M, et al. Preparation of epoxidized novolac resin nanocomposites: physical and chemical incorporation of modified graphene oxide layers for

improvement of thermal stability. *Polym Test* 2018; 68: 467–474.
21. Wu XF, Zhao YK, Zhao ZH, et al. Graphene oxide-carbon nanotubes hybrids: preparation, characterization, and application in phenol formaldehyde resin. *J Macromol Sci Part B Phys* 2015; 54: 1507–1514.
22. Abedi S, Abdouss M, Daftari-Besheli M, et al. PE/clay nanocomposite with bimodal molecular weight distribution produced via in-situ polymerization. *J Inorg Organomet Polym* 2014; 24: 416–423.
23. Yang Y, Li S, Yang W, et al. In situ polymerization deposition of porous conducting polymer on reduced graphene oxide for gas sensor. *ACS Appl Mater Interfaces* 2014; 6: 13807–13814.
24. Soleimani H, Bagheri R and Asadinezhad A. Effect of silica nanoparticles on surface properties, particle size, and distribution of poly (methyl methacrylate-co-butyl acrylate-co-acrylic acid) synthesized by in situ emulsion polymerization. *Prog Org Coatings* 2019; 129: 278–284.
25. Shen XJ, Yang S, Shen JX, et al. Improved mechanical and antibacterial properties of silver-graphene oxide hybrid/polylactid acid composites by in-situ polymerization. *Ind Crops Prod* 2019; 130: 571–579.
26. Zhao X, Li Y, Chen W, et al. Improved fracture toughness of epoxy resin reinforced with polyamide 6/graphene oxide nanocomposites prepared via in situ polymerization. *Compos Sci Technol* 2019; 171: 180–189.
27. Ahmadi Y, Yadav M and Ahmad S. Oleo-polyurethane-carbon nanocomposites: effects of in-situ polymerization and sustainable precursor on structure, mechanical, thermal, and antimicrobial surface-activity. *Compos Part B Eng* 2019; 164: 683–692.
28. Oh H and Kim J. Fabrication of polymethyl methacrylate composites with silanized boron nitride by in-situ polymerization for high thermal conductivity. *Compos Sci Technol* 2019; 172: 153–162.
29. Cuentas-Gallegos AK, Martínez-Rosales R, Rincón ME, et al. Design of hybrid materials based on carbon nanotubes and polyoxometalates. *Opt Mater (Amst)* 2006; 29: 126–133.
30. Smith B, Wepasnick K, Schrote KE, et al. Influence of surface oxides on the colloidal stability of multi-walled carbon nanotubes: a structure-property relationship. *Langmuir* 2009; 25: 9767–9776.
31. Avilés F, Cauich-Rodríguez JV, Moo-Tah L, et al. Evaluation of mild acid oxidation treatments for MWCNT functionalization. *Carbon N Y* 2009; 47: 2970–2975.
32. Haydar S, Moreno-Castilla C, Ferro-García MA, et al. Regularities in the temperature-programmed desorption spectra of CO_2 and CO from activated carbons. *Carbon N Y* 2000; 38: 1297–1308.
33. Osorio AG, Silveira ICL, Bueno VL, et al. H2SO4/HNO3/HCl-Functionalization and its effect on dispersion of carbon nanotubes in aqueous media. *Appl Surf Sci* 2008; 255: 2485–2489.
34. Sezer N and Koç M. Oxidative acid treatment of carbon nanotubes. *Surfaces Interfaces* 2019; 14: 1–8.
35. Zhang J, Zou H, Qing Q, et al. Effect of chemical oxidation on the structure of single-walled carbon nanotubes – the journal of physical chemistry B (ACS publications). *J Phys Chem B* 2003; 107: 3712–3718.
36. Saleh TA. The influence of treatment temperature on the acidity of MWCNT oxidized by HNO3 or a mixture of HNO3/H2SO4. *Appl Surf Sci* 2011; 257: 7746–7751.
37. Zhang L, Zhang Y, Wang L, et al. Phenolic resin modified by boron-silicon with high char yield. *Polym Test* 2019; 73: 208–213.
38. Saghar A, Khan M, Sadiq I, et al. Effect of carbon nanotubes and silicon carbide particles on ablative properties of carbon fiber phenolic matrix composites. *Vacuum* 2018; 148: 124–126.
39. Sandhya P. k, Sreekala M. s, Padmanabhan M, et al. Effect of starch reduced graphene oxide on thermal and mechanical properties of phenol formaldehyde resin nanocomposites. *Compos Part B Eng* 2019; 167: 83–92.
40. Sreekala MS, Kumaran MG, Joseph R, et al. Stress-relaxation behaviour in composites based on short oil-palm fibres and phenol formaldehyde resin. *Compos Sci Technol* 2001; 61: 1175–1188.
41. Sreekala MS, George J, Kumaran MG, et al. The mechanical performance of hybrid phenol-formaldehyde-based composites reinforced with glass and oil palm fibres. *Compos Sci Technol* 2002; 62: 339–353.
42. Zhou C, Wang S, Zhuang Q, et al. Enhanced conductivity in polybenzoxazoles doped with carboxylated multi-walled carbon nanotubes. *Carbon N Y* 2008; 46: 1232–1240.
43. Li X, Huang YD, Liu L, et al. Preparation of multiwall carbon nanotubes/poly(p-phenylene benzobisoxazole) nanocomposites and analysis of their physical properties. *J Appl Polym Sci* 2006; 102: 2500–2508.
44. Goyanes S, Rubiolo GR, Salazar A, et al. Carboxylation treatment of multiwalled carbon nanotubes monitored by infrared and ultraviolet spectroscopies and scanning probe microscopy. *Diam Relat Mater* 2007; 16: 412–417.
45. Nie P, Min C, Song HJ, et al. Preparation and tribological properties of polyimide/carboxyl-functionalized multi-walled carbon nanotube nanocomposite films under seawater lubrication. *Tribol Lett* 2015; 58: 1–12.
46. Chang YH, Wu MS and Lin KF. Graphting polyimide to MWCNT for enhancing dispersion and properties of MWCNT/polyetherimide nanocomposites. *J Polym Res* 2014; 21: 419.
47. Tian C, Yu-Zhou W, Hai-Hui L, et al. Melt-spinning of carboxylated MWNTs-reinforced polyamide 6 fibers with solid mixing nanocomposites. *Polym Compos* 2018; 39: 4298–4309.
48. Braun EI and Pantano P. The importance of an extensive elemental analysis of single-walled carbon nanotube soot. *Carbon N Y* 2014; 77: 912–919.
49. Plata DL, Gschwend PM and Reddy CM. Industrially synthesized single-walled carbon nanotubes: compositional data for users, environmental risk assessments, and source apportionment. *Nanotechnology* 2008; 19: 185706.

50. Lee GW, Kim J, Yoon J, et al. Structural characterization of carboxylated multi-walled carbon nanotubes. *Thin Solid Films* 2008; 516: 5781–5784.
51. Cernik RJ. *X-ray powder diffractometry*. *An introduction*. (Serie: Chemical Analysis, Vol. 138.) VonR. Jenkins undR. L. Snyder. New York: John Wiley & Sons, 1996.
52. Price GJ, Nawaz M, Yasin T, et al. Sonochemical modification of carbon nanotubes for enhanced nanocomposite performance. *Ultrason Sonochem* 2018; 40: 123–130.
53. Fashedemi OO, Miller HA, Marchionni A, et al. Electrooxidation of ethylene glycol and glycerol at palladium-decorated FeCo@Fe core-shell nanocatalysts for alkaline direct alcohol fuel cells: functionalized MWCNT supports and impact on product selectivity. *J Mater Chem A* 2015; 3: 7145–7156.
54. Okpalugo TIT, Papakonstantinou P, Murphy H, et al. High resolution XPS characterization of chemical functionalised MWCNTs and SWCNTs. *Carbon N Y* 2005; 43: 153–161.
55. Naeimi H, Mohajeri A, Moradi L, et al. Efficient and facile one pot carboxylation of multiwalled carbon nanotubes by using oxidation with ozone under mild conditions. *Appl Surf Sci* 2009; 256: 631–635.
56. Ayatollahi MR, Shadlou S, Shokrieh MM, et al. Effect of multi-walled carbon nanotube aspect ratio on mechanical and electrical properties of epoxy-based nanocomposites. *Polym Test* 2011; 30: 548–556.
57. Zhao X, Zhang Q, Chen D, et al. Enhanced mechanical properties of graphene-based polyvinyl alcohol composites. *Macromolecules* 2010; 43: 2357–2363.
58. Wu XF, Zhao YK, Zhang Y, et al. The comparison of mechanical and thermal properties of carbon nanotubes and graphene naonosheets enhanced phenol-formaldehyde resin. *J Chem Soc Pakistan* 2017; 39: 737–742.
59. Zhang W, Picu RC and Koratkar N. The effect of carbon nanotube dimensions and dispersion on the fatigue behavior of epoxy nanocomposites. *Nanotechnology* 2008; 19: 285709.
60. Zheng N, Sun W, Liu HY, et al. Effects of carboxylated carbon nanotubes on the phase separation behaviour and fracture-mechanical properties of an epoxy/polysulfone blend. *Compos Sci Technol* 2018; 159: 180–188.
61. Tamore MS, Ratna D, Mishra S, et al. Effect of functionalized multi-walled carbon nanotubes on physicomechanical properties of silicone rubber nanocomposites. *J Compos Mater* 2019; 53: 3157–3168.
62. Gu H, Zhang H, Ma C, et al. Trace electrosprayed nanopolystyrene facilitated dispersion of multiwalled carbon nanotubes: simultaneously strengthening and toughening epoxy. *Carbon N Y* 2019; 142: 131–140.
63. Hoa LTM. Characterization of multi-walled carbon nanotubes functionalized by a mixture of HNO3/H2SO4. *Diam Relat Mater* 2018; 89: 43–51.
64. Moreno-Castilla C, Carrasco-Marín F, Maldonado-Hódar FJ, et al. Effects of non-oxidant and oxidant acid treatments on the surface properties of an activated carbon with very low ash content. *Carbon N Y* 1998; 36: 145–151.
65. Chao M, Li Y, Wu G, et al. Functionalized multiwalled carbon nanotube-reinforced polyimide composite films with enhanced mechanical and thermal properties. *Int J Polym Sci* 2019; 2019: 1–12.
66. Loos MR, Coelho LAF, Pezzin SH, et al. Effect of carbon nanotubes addition on the mechanical and thermal properties of epoxy matrices. *Mat Res* 2008; 11: 347–352.
67. Zhou YX, Wu PX, Cheng ZY, et al. Improvement in electrical, thermal and mechanical properties of epoxy by filling carbon nanotube. *Express Polym Lett* 2008; 2: 40–48.
68. Ciecierska E, Boczkowska A, Kurzydlowski KJ, et al. The effect of carbon nanotubes on epoxy matrix nanocomposites. *J Therm Anal Calorim* 2013; 111: 1019–1024.
69. Pujari PK, Sudarshan K, Sharma SK, et al. Effect of interfacial interaction on free volumes in phenol-formaldehyde resin–carbon nanotube composites: positron annihilation lifetime and age momentum correlation studies. *Phys Chem Chem Phys* 2012; 14: 10972.
70. Manoharan MP, Sharma A, Desai AV, et al. The interfacial strength of carbon nanofiber epoxy composite using single fiber pullout experiments. *Nanotechnology* 2009; 20: 295701.
71. Coleman JN, Khan U, Blau WJ, et al. Small but strong: a review of the mechanical properties of carbon nanotube-polymer composites. *Carbon N Y* 2006; 44: 1624–1652.
72. Yaghoobi H and Fereidoon A. Preparation and characterization of short kenaf fiber-based biocomposites reinforced with multi-walled carbon nanotubes. *Compos Part B Eng* 2019; 162: 314–322.
73. Jiang Z, Zhang H, Han J, et al. Percolation model of reinforcement efficiency for carbon nanotubes dispersed in thermoplastics. *Compos Part A Appl Sci Manuf* 2016; 86: 49–56.
74. Abraham J, Mohammed Arif P, Kailas L, et al. Developing highly conducting and mechanically durable styrene butadiene rubber composites with tailored microstructural properties by a green approach using ionic liquid modified MWCNTs. *RSC Adv* 2016; 6: 32493–32504.